Low-profile Dual-polarized Filtering Antenna with Improved Gain and Impedance Bandwidth using Characteristic Mode Analysis

Zong-Zhuo Wang[1], Neng-Wu Liu[1*], and Liang Fang[2]

[1]National Key Laboratory of Antennas and Microwave Technology
Xidian University, Xi'an, 710071, China
zzhwang@stu.xidian.edu.cn, *yb47448@umac.mo

[2]Aviation Key Lab of Science and Technology on High Performance Electromagnetic Windows AVIC Research
Institute for Special Structures of Aeronautical Composites, Ji'nan, Shandong, 250023, China
fangl005@avic.com

Abstract – A low-profile dual-polarized filtering microstrip patch antenna (MPA) with improved gain and bandwidth is realized without requirement of filtering circuit. Herein, the characteristic mode analysis (CMA) method is adopted to analyze the antenna performances. Initially, the resonant modes of the MPA are deeply analyzed, which indicates that its resonant frequencies of CM1 and CM3 could be moved close to each other by loading slots and shorting pins, thus broadening the impedance bandwidth. Then, the influence of the slots on radiation patterns of the antenna is further studied. The results demonstrate that the non-broadside radiation beam of its CM1 could be reshaped as the broadside beam, and the sidelobe level of its CM3 could be reduced by cutting the slots, leading to the improved gain. After that, the effect of the pins on the gain-response is investigated, It shows that the gain nulls of the MPA could be controlled at both lower and upper bands, especially for the non-filtering scheme. Finally, the proposed dual-polarized antenna is fabricated and tested. The results prove that its impedance bandwidth reaches to about 7.4% with a low-profile of about 0.038 free-space wavelength. Besides, a stable enhanced gain of around 10 dBi is achieved over the operating band.

Index Terms – Characteristic mode analysis (CMA), filtering response, high-gain, low-profile, non-filtering scheme.

I. INTRODUCTION

With the rapid development of wireless communication technology, communication systems tend to be miniaturized, integrated, and multifunctional. In order to reduce the interference between the antennas of different frequency bands in the communication system, and to meet the system miniaturization, it is more meaningful to integrate the filter with antenna design.

In recent years, more extensive research and design of filter antennas have been carried out. Firstly, one approach is to cascade the filter and the antenna, with the antenna radiator as the last stage of the filter [1–4]. This cascading method requires the separation of the feeding part and the antenna, which is not conducive to the miniaturization of the antenna. At the same time, due to the existence of the filter, the antenna still has transmission loss, which will deteriorate the radiation gain of the antenna. Secondly, incorporating or embedding filtering structures into the original antenna is a mainstream design approach. For example, the filtering performance is obtained by adopting novel feeding structures [5–10] and loading same-layer or stacked parasitic elements [11–17]. However, the above methods increase the complexity of the design and still have the problems of large size and high profile of the antenna. A more efficient method is to slot or load shorting pins in the antenna to obtain one or more radiation gain nulls [18–24]. This greatly simplifies the complexity of the antenna design while maintaining the characteristics of miniaturization and low profile. The dual-polarization design of the filtering antenna will improve the capability of the antenna, alleviate the polarization mismatch problem caused by the multipath effects, and improve the utilization rate of spectrum resources.

In this paper, a novel dual-polarized filtering antenna is proposed with no extra filtering circuit and high gain. While maintaining the low-profile characteristics, the filtering response is obtained by loading the shorting pins, and the frequency band is widened by the combination of the loading the shorting pins and slotting.

II. GEOMETRY AND WORKING PRINCIPLE

The configuration of the proposed low-profile dual-polarized filtering microstrip patch antenna (MPA) with improved gain and impedance bandwidth is depicted in

Fig. 1. It shows that a radiating patch with the dimensions of $L_1 \times L_1$ is printed on the top surface of a substrate ($L \times L$), which has the thickness $H_1 = 0.8$ mm, loss tangent of about 0.001, and dielectric constant $\varepsilon r1 = 2.17$.
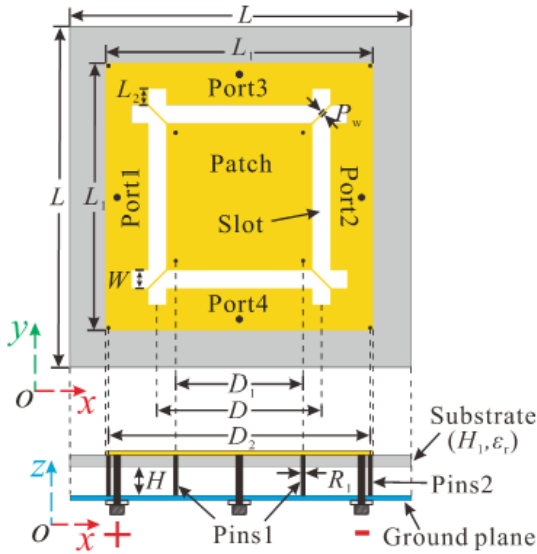

Fig. 1. Configuration of the proposed dual-polarized filtering MPA: $L = 160$, $L_1 = 120$, $L_2 = 4$, $W = 9$, $H = 4$, $H_1 = 0.8$, $D = 78$, $D_1 = 60$, $D_2 = 118$, $P_w = 0.4$, $R_1 = 0.2$. Unit: mm.
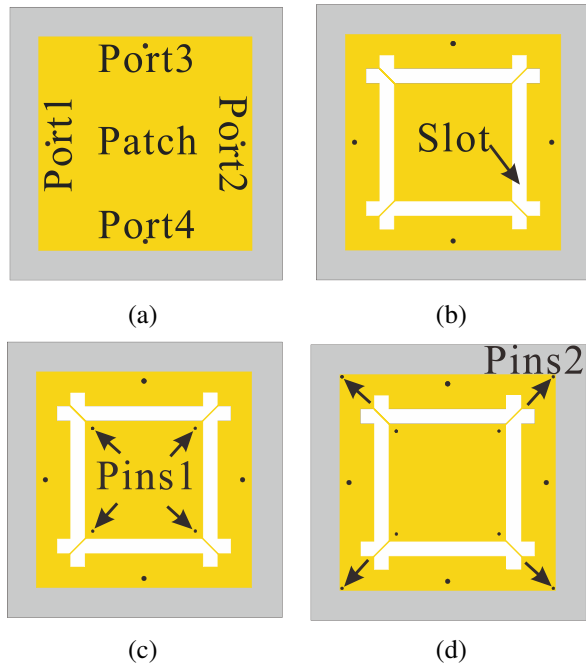

Fig. 2. Evolution process of our proposed MPA: (a) Antenna I, (b) antenna II, (c) antenna III, and (d) the proposed antenna.

Besides, the ground plane ($L \times L$) is placed below the substrate with an air gap of $H = 4$ mm. Figure 2 gives an evolution process of the MPA. By loading two pairs of bent slots with spacing D, the desired CM1 and CM3 could be shifted close to each other, and it also contributes to improve the radiation beams of these two modes. In addition, four shorting pins are loaded inside antenna II to generate the radiation gain null at the upper band, while four shorting pins are loaded on the edge of antenna III to generate the radiation gain null at the lower band. In the following, the proposed MPA is extensively analyzed with all the simulated results to be provided.

A. Mode selection

Initially, characteristic mode analysis (CMA) is used to select the desired modes of the traditional MPA for simultaneous gain and bandwidth enhancements. Note that the following analyses, conducted as port 1 and port 2, are excited differentially. Figure 3 plots the modal significance (MS) and modal weighting coefficient (MWC) of antenna I. As can be seen, there are four resonant modes (CM1, CM2, CM3, and CM4) in the wide frequency band. As such, the corresponding electric fields and radiation patterns of these four modes are illustrated in Figs. 4 and 5. It shows that only CM3 has the maxi-
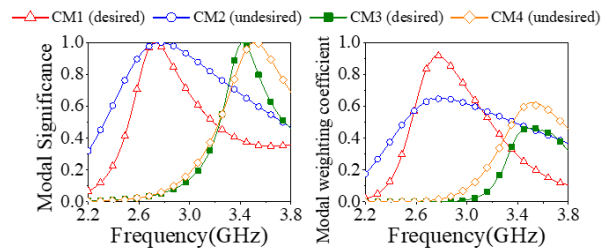

Fig. 3. Modal significance and modal weighting coefficient of the antenna I.
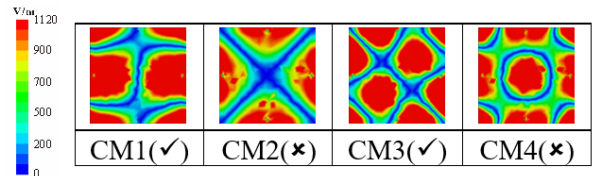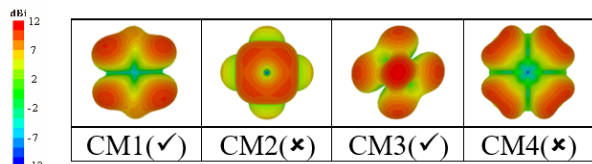

Fig. 4. Modal electric fields of the antenna I.

Fig. 5. Modal radiation patterns of the antenna I.

mum gain in the normal direction, while the other modes have radiation nulls in this direction. Most importantly, the maximum gains of its CM1, CM2, CM3, and CM4 reach to about 9.77 dBi, 8.87 dBi, 12.1 dBi, and 8.99 dBi, respectively. Hence, CM1 and CM3 are selected as the desired modes for the realization of wide-bandwidth and high-gain simultaneously.

B. Gain improvement

The results Fig. 5 indicate that CM1 suffers from the non-broadside radiation beam, and the CM3 simultaneously has a high sidelobe level. Hence, in order to reshape radiated fields of these dual modes, a set of four slots are cut on the radiating patch as shown in Fig. 2 (b) or Fig. 6. Due to the symmetrical loaded slots, these four slots will cross each other when they reach a large length and therefore are bent.
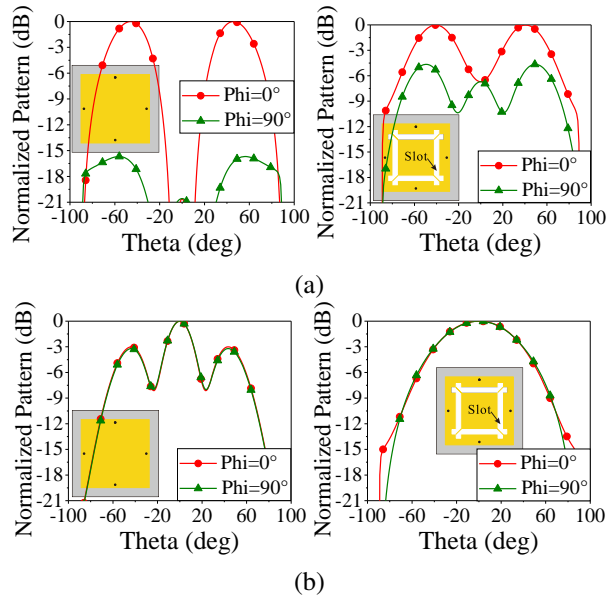

(a)

(b)

Fig. 6. Normalized patterns of the MPA with and without the slots: (a) CM1 and (b) CM3.

Besides, the normalized radiation patterns of the MPA with and without these slots are compared under these two modes (see Fig. 6). As can be seen in Fig. 6, the gain of the antenna in the broadside direction could be enhanced by loading these slots at CM1. This working principle has been proven from the previous works [25–26]. Meanwhile, the sidelobe level of its CM3 could be gradually reduced from 3.2 dB to 0 dB via these components.

C. Filtering response generation

Apart from gain improvement, the antenna with filtering response is in high demand. As shown in Fig. 7, when four shorting pins1 are loaded around the diagonal position inside antenna II, the resonant frequency

of CM3 could be shifted up significantly to a high frequency band as compared to that of CM1. As such, the dual modes are successfully moved close to each other.

The peak realized gain curves of the antennas with and without the loaded pins1 are illustrated in Fig. 8, where it can be seen that a radiation gain null in the upper band is generated by loading the pins1. To be extended, the electric current distributions of antenna II and antenna III are compared in Fig. 9. Compared with antenna II, the current inside the antenna III undergoes a reversal after loading the pins1. At this point, along the x-axis or y-axis, the surface current flows symmetrically in the opposite direction, which results in the far-field radiation of the antenna to be cancelled out in the broadside direction, thus generating a radiation null in the upper band.
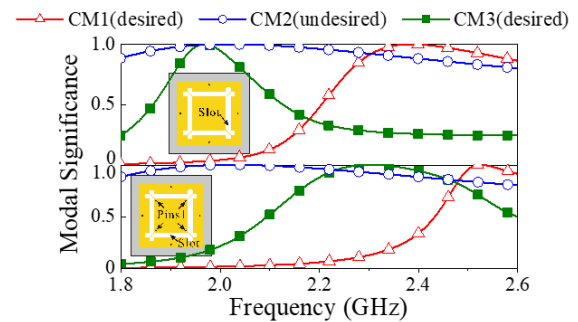

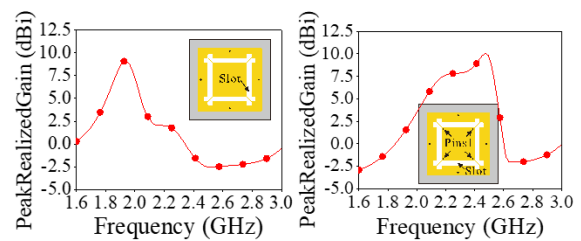Fig. 7. Modal significance of the MPA with and without the loaded pins1.

Fig. 8. Peak realized gain curves of the MPA with and without the loaded pins1.
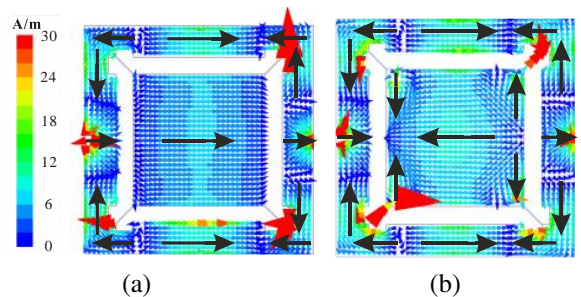

(a)   (b)

Fig. 9. Electric current distribution on the patch at 2.7 GHz for (a) antenna II and (b) antenna III.

After that, the effect of four shorting pins2 on the resonant frequencies of antenna III is further studied. As can be seen from Fig. 10, the frequency spacing between two modes is further reduced. By comparing the peak realized gain curves before and after loading pins2, it can be found in Fig. 11 that a new radiation gain null in the lower band is generated.

Moreover, the electric current distributions of antenna III and the proposed antenna are compared in Fig. 12. It can be seen that there is almost no current distribution inside the two antennas, but the current at the edge of the proposed antenna has changed. At this point, the current at the edge of the antenna flows symmetrically and reversely along the y-axis, and the current along

the x-axis is offset by the current in the diagonal direction, which results in the far-field radiation of the antenna to cancel out in the broadside direction, thus generating a radiation gain null in the lower band.

III. RESULTS AND EXPERIMENTAL VALIDATION

To validate the performance mentioned above, the proposed antenna is fabricated and measured, with the prototype shown in Fig. 13. Initially, the $|S_{dd11}|$ of our proposed antenna is measured by using the R&S ZNB20 Vector Network Analyzer, and the relevant simulated and measured results are presented in Fig. 14. As can be seen, the measured S-parameter is matched well with the simulated S-parameter under the two polarization operations. The impedance bandwidth of the proposed antenna for $|S_{dd11}| < $ -10 dB is 7.4% ranging from 2.34 to 2.52 GHz.

After that, the radiation patterns, peak realized gains, and radiation efficiencies of the proposed antenna are measured by employing a near-field SATIMO antenna test system. As shown in Fig. 15, the measured radiation patterns are in good agreement with the simulated radiation patterns at 2.37 and 2.49 GHz, and the cross-polarization is lower than -20 dB.

In addition, the simulated and measured peak realized gains and radiation efficiencies of the proposed antenna are presented in Fig. 16. As can be seen, the
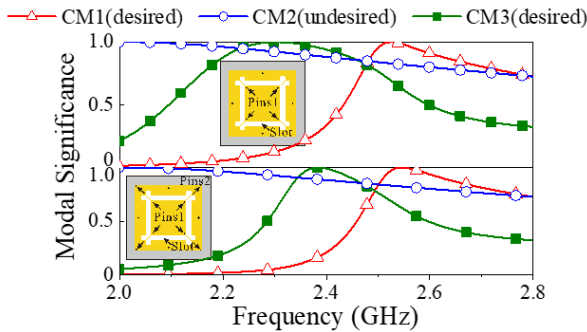

Fig. 10. Modal significance of the antenna with and without the loaded pins2.
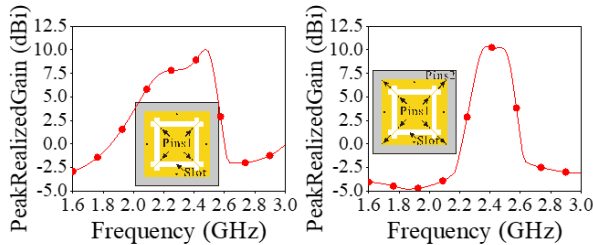

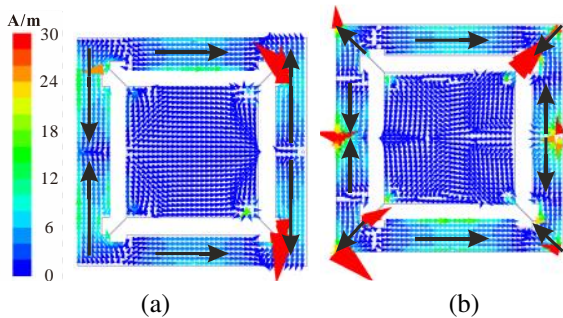Fig. 11. Modal significance of the antenna with and without the loaded pins2.

Fig. 12. Electric current distribution on the patch at 1.9 GHz for (a) antenna III and (b) proposed antenna.
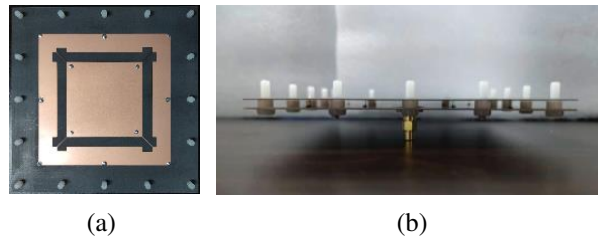

(a) (b)

Fig. 13. Photograph of the fabricated MPA: (a) Top view and (b) side view.
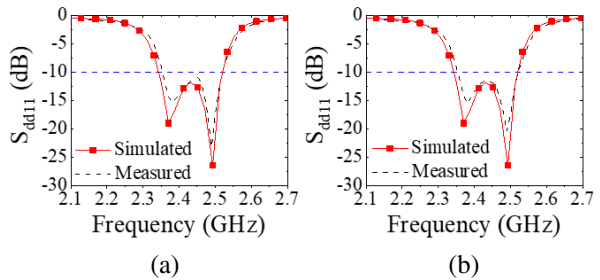

(a) (b)

Fig. 14. Simulated and measured S-parameter of the proposed antenna: (a) Port 1 and port 2 are differentially excited and (b) port 3 and port 4 are differentially excited.

Table 1: Performance comparison with the previous filtering antennas

| Ref.	Polarization	Filtering Method	Radiator Volume	Gain (dBi)	Extra Filtering Circuit	Easy for Integration
[10]	single	Filtering circuit	$0.056\lambda_0^3 \uparrow$	$8.7 \downarrow$	Yes	No
[11]	single	Stacked patch + Slots	$0.13\lambda_0^3 \uparrow$	$7.2 \downarrow$	No	No
[5], [7]	dual	Filtering circuit	$\geq 0.145\lambda_0^3 \uparrow$	$\approx 8dBi \downarrow$	Yes	No
[8]	dual	Filtering circuit	$0.022\lambda_0^3$	$8.8dBi \downarrow$	Yes	Yes
[12], [16]	dual	Stacked patch	$\geq 0.095\lambda_0^3 \uparrow$	$\approx 9.2dBi \downarrow$	No	No
[15]	dual	Stacked patch	$0.036\lambda_0^3 \uparrow$	$5.2dBi \downarrow$	No	No
[20], [22]	dual	Slots + Pins	$0.144\lambda_0^3 \uparrow$	$9.5dBi \downarrow$	No	Yes
[21], [24]	dual	Slots	$0.137\lambda_0^3 \uparrow$	$9.5dBi \downarrow$	No	No
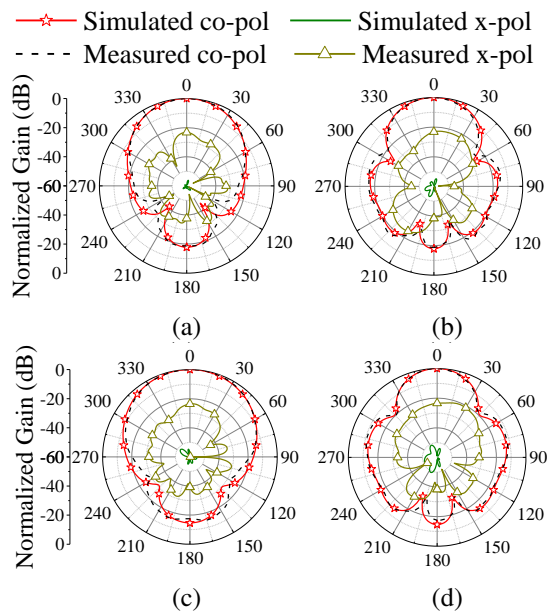
Fig. 15. Simulated and measured radiation patterns of the proposed antenna: (a) xoz plane at 2.37 GHz, (b) yoz plane at 2.37 GHz, (c) xoz plane at 2.49 GHz, and (d) yoz plane at 2.49 GHz.

Fig. 16. Simulated and measured gains and efficiencies of the proposed antenna.

antenna has obtained a stable peak gain of around 10.1 dBi in the operating frequency band, and the radiation efficiency of the antenna is around 90%. Hence, the proposed antenna has the single-layer, low-profile (0.038 λ_0), high-gain properties as desired without extra feeding networks.

Finally, a comparison between the proposed antenna and previous filtering antennas is presented in Table 1. The antennas in [10–11] exhibit good single-polarization filtering performance but cannot meet the requirements in a multi-polarization scenario. The antennas in [5], [7], and [8] achieved good filtering performance through the design of extra filter circuits, but these filter circuits increase design complexity and introduce insertion loss.
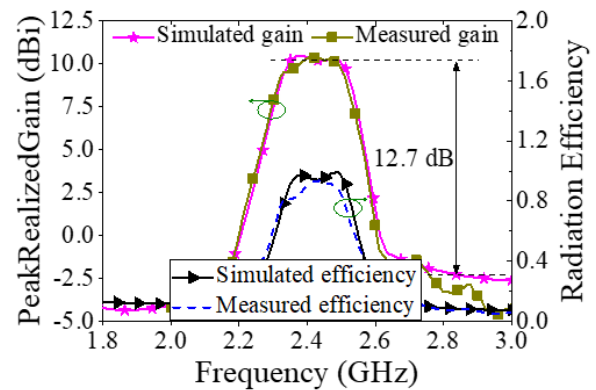
Additionally, the antennas in [12], [15], and [16] use the method of adding stacked patches to obtain good filtering performance, but they are not suitable for integration. Both the antenna proposed by us and the antennas in [20–22] and [24] achieve good filtering performance by slotting or loading shorting pins, and no extra filtering circuit is used. However, our proposed antenna has more advantages in terms of radiator volume and gain.

IV. CONCLUSION

In this paper, a novel dual-polarized filtering antenna without extra filtering circuit is proposed. Initially, the desired operating mode is selected by analyzing the electric field and radiation field of each characteristic mode. Next, the frequency spacing between the selected modes is reduced by slotting, and the radiation pattern with radiation nulls in broadside direction is improved. Finally, without using extra filter circuits, two flexibly controllable radiation nulls are introduced by loading the shorting pins inside the antenna and at the edge of the antenna, thus to achieve the wide impedance bandwidth and filtering performance of the realized gain simultaneously. The measured results indicate that the antenna has an

impedance bandwidth of 7.4% in the range of 2.34 - 2.52 GHz, and a stable peak gain of 10.1 ± 0.45 dBi is obtained in the operating frequency band. In particular, the characteristics of low profile ($0.038 \lambda_0$) and no extra filtering circuit make this antenna a good candidate for dual-polarization filtering applications.

ACKNOWLEDGMENT

REFERENCES

[1] C.-X. Mao, S. Gao, Y. Wang, F. Qin, and Q.-X. Chu, "Multimode resonator-fed dual-polarized antenna array with enhanced bandwidth and selectivity," *IEEE Trans. Antennas Propag.*, vol. 63, no. 12, pp. 5492-5499, Dec. 2015.

[2] W.-J. Wu, Y.-Z. Yin, S.-L. Zuo, Z.-Y. Zhang, and J.-J. Xie, "A new compact filter-antenna for modern wireless communication systems," *IEEE Antennas Wireless Propag. Lett.*, vol. 10, pp. 1131-1134, 2011.

[3] J.-F. Li, D.-L. Wu, G. Zhang, Y.-J. Wu, and C.-X. Mao, "Compact dual-polarized antenna for dual-band full-duplex base station applications," *IEEE Access.*, vol. 7, pp. 72761-72769, 2019.

[4] C.-X. Mao, S. Gao, Y. Wang, Q. Luo, and Q.-X. Chu, "A shared-aperture dual-band dual-polarized filtering-antenna-array with improved frequency response," *IEEE Trans. Antennas Propag.*, vol. 65, no. 4, pp. 1836-1844, Apr. 2017.

[5] Y. Zhang, X. Y. Zhang, L. Gao, Y. Gao, and Q. H. Liu, "A two-port microwave component with dual-polarized filtering antenna and single-band bandpass filter operations," *IEEE Trans. Antennas Propag.*, vol. 67, no. 8, pp. 5590-5601, Aug. 2019.

[6] Y. Li, Z. Zhao, Z. Tang, and Y. Yin, "Differentially fed, dual-band dual-polarized filtering antenna with high selectivity for 5G sub-6 GHz base station applications," *IEEE Trans. Antennas Propag.*, vol. 68, no. 4, pp. 3231-3236, Apr. 2020.

[7] S. J. Yang, Y. F. Cao, Y. M. Pan, Y. Wu, H. Hu, and X. Y. Zhang, "Balun-fed dual-polarized broadband filtering antenna without extra filtering structure," *IEEE Antennas Wireless Propag. Lett.*, vol. 19, no. 4, pp. 656-660, Apr. 2020.

[8] J. Liu, H. Liu, X. Dou, Y. Tang, C. Zhang, L. Wang, R. Tang, and Y. Yin, "A low profile, dual-band, dual-polarized patch antenna with antenna-filter functions and its application in MIMO systems," *IEEE Access.*, vol. 9, pp. 101164-101171, 2021.

[9] W. Duan, Y. F. Cao, Y.-M. Pan, Z. X. Chen, and X. Y. Zhang, "Compact dual-band dual-polarized base-station antenna array with a small frequency ratio using filtering elements," *IEEE Access.*, vol. 7, pp. 127800-127808, 2019.

[10] P. F. Hu, Y. M. Pan, X. Y. Zhang, and S. Y. Zheng, "Broadband filtering dielectric resonator antenna with wide stopband," *IEEE Trans. Antennas Propag.*, vol. 65, no. 4, pp. 2079-2084, Apr. 2017.

[11] K. Xu, J. Shi, X. Qing, and Z. N. Chen, "A substrate integrated cavity backed filtering slot antenna stacked with a patch for frequency selectivity enhancement," *IEEE Antennas Wireless Propag. Lett.*, vol. 17, no. 10, pp. 1910-1914, Oct. 2018.

[12] W. Duan, X. Y. Zhang, Y.-M. Pan, J.-X. Xu, and Q. Xue, "Dual-polarized filtering antenna with high selectivity and low cross polarization," *IEEE Trans. Antennas Propag.*, vol. 64, no. 10, pp. 4188-4196, Oct. 2016.

[13] Y. Liu, S. Wang, N. Li, J.-B. Wang, and J. Zhao, "A compact dual-band dual-polarized antenna with filtering structures for sub-6 GHz base station applications," *IEEE Antennas Wireless Propag. Lett.*, vol. 17, no. 10, pp. 1764-1768, Oct. 2018.

[14] C. F. Ding, X. Y. Zhang, and M. Yu, "Simple dual-polarized filtering antenna with enhanced bandwidth for base station applications," *IEEE Trans. Antennas Propag.*, vol. 68, no. 6, pp. 4354-4361, June 2020.

[15] S. J. Yang, Y. M. Pan, L.-Y. Shi, and X. Y. Zhang, "Millimeter-wave dual-polarized filtering antenna for 5G application," *IEEE Trans. Antennas Propag.*, vol. 68, no. 7, pp. 5114-5121, July 2020.

[16] C. Hua, R. Li, Y. Wang, and Y. Lu, "Dual-polarized filtering antenna with printed Jerusalem-cross radiator," *IEEE Access.*, vol. 6, pp. 9000-9005, 2018.

[17] Y. Zhang, Y. Zhang, D. Li, Z. Niu, and Y. Fan, "Dual-polarized low-profile filtering patch antenna without extra circuit," *IEEE Access.*, vol. 7, pp. 106011-106018, 2019.

[18] Y. Y. Liu, X. Y. Zhang, and S. J. Yang, "Compact dual-band dual-polarized filtering antenna for 5G base station applications," *Proc. Int. Symp. Antennas Propag. (ISAP)*, pp. 791-792, 2021.

[19] Y. F. Cao, X. Y. Zhang, and Q. Xue, "Compact shared-aperture dual-band dual-polarized array

using filtering slot antenna and dual-function meta-surface," *IEEE Trans. Antennas Propag.*, vol. 70, no. 2, pp. 1120-1131, Feb. 2022.

[20] W. Yang, M. Xun, W. Che, W. Feng, Y. Zhang, and Q. Xue, "Novel compact high-gain differential-fed dual-polarized filtering patch antenna," *IEEE Trans. Antennas Propag.*, vol. 67, no. 12, pp. 7261-7271, Dec. 2019.

[21] K. Xue, D. Yang, C. Guo, H. Zhai, H. Li, and Y. Zeng, "A dual-polarized filtering base-station antenna with compact size for 5G applications," *IEEE Antennas Wireless Propag. Lett.*, vol. 19, no. 8, pp. 1316-1320, Aug. 2020.

[22] Y. Q. Sun, Z. J. Zhai, D. H. Zhao, F. Lin, X. Y. Zhang, and H. J. Sun, "High-gain low cross-polarized dual-polarized filtering patch antenna without extra circuits," *IEEE Antennas Wireless Propag. Lett.*, vol. 21, no. 7, pp. 1368-1372, July 2022.

[23] S. J. Yang, Y. M. Pan, Y. Zhang, Y. Gao, and X. Y. Zhang, "Low-profile dual-polarized filtering magneto-electric dipole antenna for 5G applications," *IEEE Trans. Antennas Propag.*, vol. 67, no. 10, pp. 6235-6243, Oct. 2019.

[24] H. Yuan, F.-C. Chen, and Q.-X. Chu, "A wideband and high gain dual-polarized filtering antenna based on multiple patches," *IEEE Trans. Antennas Propag.*, May 2022.

[25] N.-W. Liu, L. Zhu, W.-W. Choi, and G. Fu, "A low-profile wideband aperture-fed microstrip antenna with improved radiation patterns," *IEEE Trans. Antennas Propag.*, vol. 67, no. 1, pp. 562-567, Jan. 2019.

[26] L. Zhu and N.-W. Liu, "Multimode resonator technique in antennas: A review," *Electromagnetic Science*, vol. 1, no. 1, pp. 1-17, Mar. 2023.

Zong-Zhuo Wang was born in Liaocheng, China. He is currently pursuing the M.E degree from Xidian University, Xi'an, China. His current research interests include low-profile antennas, filtering antennas, and multifunctional antennas.

Neng-Wu Liu was born in Changde, China. Since 2018, he has been an associate professor with Xidian University. His current research interests include the designs of antenna theory, low-profile antennas, multimode antennas, wideband antennas, patch antennas, filtering antennas, and phased arrays.

Liang Fang was born in 1986, and he is a senior engineer at the AVIC Research Institute for Special Structures of Aeronautical Composites. His current research focuses on radio propagation and comprehensive design of electromagnetic windows.